ADVANCED MATERIALS

Supporting Information

for *Adv. Mater.*, DOI: 10.1002/adma. 201303657

Broadband All-Dielectric Magnifying Lens for Far-Field High-Resolution Imaging

Wei Xiang Jiang, Cheng-Wei Qiu, Tian Cheng Han, Qiang Cheng, Hui Feng Ma, Shuang Zhang, and Tie Jun Cui**

Supporting Information

for *Adv. Mater.*, DOI: 10.1002/adma.201300226

Broadband all-dielectric magnifying lens for far-field high resolution imaging

By *Wei Xiang Jiang, Cheng-Wei Qiu*, Tian Cheng Han, Qiang Cheng, Hui Feng Ma, Shuang Zhang, and Tie Jun Cui**

1. Derivation of the transformation-optics magnifying lens

To compress the circular region ($r' \le b-\delta$) in the virtual space into region I ($r \le a$) in the real space, the following transformation can be used

$$r = \frac{a}{b-\delta} r', \ \phi = \phi', \ z = z' \tag{1}$$

Then, the relative constitutive parameters for the core region $(r \le a)$ are expressed as

$$\varepsilon = u = diag\left(1, 1, \left(\frac{b-\delta}{a}\right)^2\right) \tag{2}$$

To stretch the annular region ($b-\delta < r' \le b$) in the virtual space into region II ($a < r \le b$) in the real space, we apply for the following transformation

$$r = \frac{b-a}{\delta}(r'-b)+b, \ \phi = \phi', \ z = z' \tag{3}$$

And the relative constitutive parameters for region II are calculated as

$$\varepsilon = u = diag\left(\frac{b-a}{\delta}\frac{r'}{r}, \frac{\delta}{b-a}\frac{r}{r'}, \frac{\delta}{b-a}\frac{r'}{r}\right) \tag{4}$$

In the two-dimensional case, we only need to consider three components (μ_r , μ_ϕ, and ε_z) for the transverse-electric polarization. Thus we can obtain

$$\mu_r = \mu_\phi = 1, \ \varepsilon_z = \left(\frac{b-\delta}{a}\right)^2 \quad \text{(for region I)} \tag{5a}$$

$$\mu_r = \frac{b-a}{\delta}\frac{r'}{r}, \ \mu_\phi = \frac{\delta}{b-a}\frac{r}{r'}, \ \varepsilon_z = \frac{\delta}{b-a}\frac{r'}{r} \quad \text{(for region II)} \tag{5b}$$

Because the wave propagation (wavenumber $\vec{k}$) is always confined in the *x*-*y* plane in the two dimensional case, Equation (5) may be replaced by the refractive index and be simplified as

$$n(r) = \begin{cases} \dfrac{b-\delta}{a} & r \le a \\ diag\left(\dfrac{\delta}{b-a}, \dfrac{r'}{r}\right) & a < r \le b \end{cases} \tag{6}$$

Assuming $\delta \to 0$, Equation (6) will be reduced to Equation (1) in the main text. The normalized far-field patterns of the transformation-optics magnifying lens at 10 GHz are shown in Figure S1, with different radial indexes of refraction

2. Imaging scheme of source positions

The imaging scheme is an inverse problem to determine the source positions ($p^{(n)}$) based on the far-field radiation patterns and the magnification factor M of the immersion lens. In fact, we can employ the inverse computation scheme to find out the equivalent positions of sources ($p_0^{(n)}$) in free space which produce the same far-field patterns. Then the actual source positions can be approximated as: $p^{(n)}= p_0^{(n)}/M$, in which n represents the index of source. In our inversion algorithm, the optimal equivalent positions of sources are determined by seeking the minized least-square norm

$$J(p_0^{(n)}) = \min\left\{\sum_i \left|F_0 - F(p_0^{(n)}, \varphi_i)\right|^2\right\}.$$

where F_0 is the known (measured or simulated) far-field patterns and $F(p_0^{(n)}, \varphi_i)$ is the calculated far-field patterns of sources positioned at $p_0^{(n)}$ in free space, which have closed-form expressions, and φ_i is the ith observation angle. In the inversion algorithm, we collect the data of electric fields along a semi-circle with the radius of 80mm. The far-field patterns are calculated from the near-field data by using the effective magnetic-current method. White noises have been added to the calculated far fields to simulate more realistic situations:

$$F = F(p_0^{(n)}, \varphi_i) + \Delta F \cdot R_{\mathrm{rand}},$$

in which ΔF is the maximum error of far fields, and R_{rand} is a random number. We note that, without white noise, breaking the diffraction limit is possible by retrieving the position of point sources from the far field.

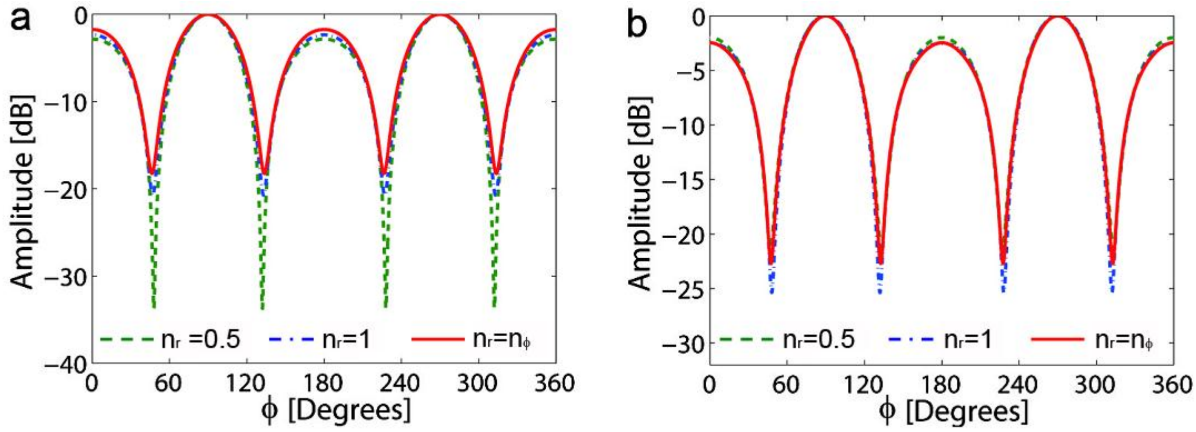

Figure S1 The normalized far-field patterns of the transformation-optics modified solid immersion lens with different radial indexes of refraction at 10 GHz. (a) The transverse-electric polarization. (b) The transverse-magnetic polarization. We observed that the far-field patterns are nearly unchanged when the radial index of refraction is set as different values for both polarizations.

3. The material parameters of the fabricated impedance-matching magnifying lens

The material parameters of the fabricated impedance-matching magnifying lens are illustrated in Table S1.

Table S1. Details of the effective permittivity and size of unit cell of the fabricated lens

<table>
<tr><td></td><td>Core Region</td><td colspan="2">Macthing Layer 1</td><td colspan="3">Macthing Layer 2</td><td colspan="3">Macthing Layer 3</td><td colspan="2">Macthing Layer 4</td><td>Macthing Layer 5</td></tr>
<tr><td>Dielectric Plate</td><td>TP2</td><td colspan="2">TP2</td><td colspan="3">FR-4</td><td colspan="3">F4B</td><td colspan="2">F4B</td><td>F4B-2</td></tr>
<tr><td>Permittivity</td><td>9.6</td><td colspan="2">9.6</td><td colspan="3">4.6</td><td colspan="3">2.65</td><td colspan="2">2.65</td><td>2.2</td></tr>
<tr><td>h (mm)</td><td>3</td><td colspan="2">3</td><td colspan="3">3</td><td colspan="3">3</td><td colspan="2">2</td><td>1</td></tr>
<tr><td>Effective Permittivity</td><td>9</td><td>7.67</td><td>5.76</td><td>4.48</td><td>3.59</td><td>2.94</td><td>2.45</td><td>2.07</td><td>1.78</td><td>1.54</td><td>1.35</td><td>1.19</td></tr>
<tr><td>D (mm)</td><td>0.8</td><td>1.4</td><td>2.1</td><td>0.5</td><td>1.7</td><td>2.3</td><td>1.2</td><td>2</td><td>2.5</td><td>1.9</td><td>2.6</td><td>1.7</td></tr>
</table>

4. Eigen-mode analysis of the magnifying lens

We introduce the rigorous theoretical analysis to the simplified modified solid immersion lens. When the transverse electric polarization is considered, the wave equation of region II can be expressed as

$$r^2\frac{\partial^2 E_z}{\partial r^2}+r\frac{\partial E_z}{\partial r}+\frac{\partial^2 E_z}{\partial \phi^2}+k_0^2 b^2 E_z=0 \tag{7}$$

where $k_0=2\pi/\lambda_0$, $n=0,\pm1,\pm2,\cdots$, and λ_0 is the wavelength in free space. Using eigenfunction expansion method, the function of *r* obviously satisfies the Euler's equation (7), and we can obtain

$$E_z^{\mathrm{II}}=\sum_{n=-\infty}^{\infty}\left[A_n\cos\left(\nu\ln r\right)+B_n\sin\left(\nu\ln r\right)\right]e^{-\mathrm{j}n\phi} \tag{8}$$

where $\nu=\sqrt{k_0^2 b^2-n^2}$, A_n and B_n are undetermined coefficients. The E_z fields of regions I and III can be expressed as

$$E_z^{\mathrm{I}}=-\frac{\omega\mu_0}{4}\sum_{n=-\infty}^{\infty}\left[1+\cos\left(n\pi\right)\right]J_n\left(k_c\frac{d}{2}\right)H_n^{(2)}\left(k_c r\right)e^{-\mathrm{j}n\phi}+\sum_{n=-\infty}^{\infty}R_n J_n\left(k_c r\right)e^{-\mathrm{j}n\phi} \tag{9}$$

$$E_z^{\mathrm{III}}=\sum_{n=-\infty}^{\infty}T_n H_n^{(2)}\left(k_0 r\right)e^{-\mathrm{j}n\phi} \tag{10}$$

where $k_c=k_0 n_c$, R_n and T_n are undetermined coefficients, and $J_n(x)$ and $H_n^{(2)}(x)$ represent the Bessel function of the first kind and the Hankel function of the second kind, respectively. According to the continuous boundary condition of tangent field components, the four unknown coefficients can be determined. Since we only concern the field in region III, T_n can be expressed as

$$T_n=\frac{\omega\mu_0}{4}\frac{\left[1+\cos(n\pi)\right]J_n(k_c\frac{d}{2})}{\cos\left(\nu\ln\frac{a}{b}\right)+Q\sin\left(\nu\ln\frac{a}{b}\right)} \tag{11}$$

where $Q=\frac{\pi k_0 b}{2\mathrm{j}}\left[\frac{\nu}{k_0 b}J_n\left(k_0 b\right)H_n^{(2)}\left(k_0 b\right)+\frac{k_0 b}{\nu}J_n'\left(k_0 b\right)H_n^{(2)\prime}\left(k_0 b\right)\right]$.

For the case of two sources with large distance, the electric field of outer region ($r>b$) can be expressed as

$$E_z^{virtual}=-\frac{\omega\mu_0}{4}\sum_{n=-\infty}^{\infty}\left[1+\cos\left(n\pi\right)\right]J_n\left(k_0.\frac{d}{2}n_c\right)H_n^{(2)}\left(k_0 r\right)e^{-\mathrm{j}n\phi} \tag{12}$$